Cluster size effects on CO oxidation activity, adsorbate affinity, and temporal behavior of model Au_n/TiO_2 catalysts

Sungsik Lee, Chaoyang Fan, Tianpin Wu, and Scott L. Anderson[a)]
Department of Chemistry, University of Utah, 315 S. 1400 E. RM Dock, Salt Lake City, Utah 84112-0850

(Received 19 April 2005; accepted 21 July 2005; published online 28 September 2005)

Model catalysts were prepared by deposition of size-selected Au_n ($n=1-7$) on rutile $TiO_2(110)$, and characterized by a combination of electron spectroscopy, ion scattering, temperature-programmed desorption, and pulse-dosing mass spectrometry. CO oxidation activity was found to vary strongly with deposited cluster size, with significant activity appearing at Au_3. Activity is not obviously correlated with affinity for CO, or with cluster morphology, but is strongly correlated with the clusters' ability to bind oxygen (during O_2 exposure) on top of the gold. The temporal dependence of CO_2 evolution in reaction of O_2 pre-exposed samples with CO pulses shows an interesting cluster size dependence. For Au_5 and Au_6, the peak CO_2 production is coincident with the peak CO flux, but for Au_3, Au_4, and Au_7, there are significant induction periods for CO_2 evolution. In addition, it is observed that some of the most active cluster sizes have the slowest CO_2 evolution rates. Several mechanistic scenarios capable of accounting for the observations are laid out. © *2005 American Institute of Physics*. [DOI: 10.1063/1.2035098]

I. INTRODUCTION

The catalytic reactivity of small size gold particles on metal oxide surfaces is one of the most interesting recent results in surface chemistry.[1–7] Because of the strong dependence of activity on particle size[1,7,8] in contrast with the inertness of bulk gold,[2,9] this system is particularly good one for testing models of size-dependence catalytic activity. Because a wide variety of reactions can be catalyzed, supported gold also is of considerable practical interest. In this paper, we focus on the CO oxidation reaction on model Au/TiO_2 catalysts, which is one of the most intensively studied reaction/gold catalyst combinations. In this system, the mechanism is complicated by strong interaction of both the Au particles and CO and O_2 reactants with the support and with oxygen vacancies in the support surface.

For high surface area Au/TiO_2 catalysts, where Au particle size was characterized by transmission electron microscopy (TEM), Haruta and co-workers found CO oxidation activity peaking for average particle sizes around 3 nm.[10] Goodman and co-workers[7] studied gold particles grown on a $TiO_2(110)$-(1×1) surface using scanning tunneling microscopy/spectroscopy (STM/STS) and CO oxidation activity measurements. They reported maximum activity for particles with average diameter around 2.5 to 3 nm with two layer thickness. Note, however, that the number of atoms in these two layer clusters was substantially smaller than in the roughly spherical TEM-visible particles in the high surface area catalyst. More recently the same group prepared gold samples on a $TiO_x/Mo(112)$ surface, where gold grew layer-by-layer, and again found maximum CO oxidation activity for samples with a gold bilayer.[11] There is also evidence that considerably smaller particles are catalytically active. For example, Fu *et al.*[12] recently showed that activity for the water gas shift reaction on Au/CeO_2 catalysts was unchanged even after the TEM-visible nanoparticles were removed, suggesting that small Au surface species were active. A more direct study was reported by Heiz and co-workers,[8] using deposition of size-selected cluster cations on MgO surfaces. They found the onset of CO oxidation activity for that system at Au_8. Recent calculations have shown that this effect is related to charging of Au cluster bound at oxygen vacancies on the surface.[13]

We recently reported a preliminary study of CO oxidation on $Au_n/TiO_2(110)$-(1×1) samples, prepared by deposition of size-selected Au_n^+.[4] Significant catalytic activity was observed starting at Au_3. In this paper, we report additional results for CO oxidation on samples prepared by Au_n^+ ($n=1-7$) deposition on a single crystal $TiO_2(110)$ surface. The size dependence of catalytic activity is characterized in more detail, and factors controlling activity are probed by examining correlations of activity with size, morphology, and the ability of the samples to chemisorb the reactants on both gold and substrate sites. Most previous ultra high vacuum (UHV) studies of CO oxidation on Au/TiO_2 have used atomic oxygen as a reactant, to avoid problems with very low sticking probability for O_2.[3,6,14] As described in our preliminary communication on this system,[4] we found that molecular oxygen can be used as the oxidant under UHV conditions, and one purpose of this paper is to investigate how O_2 binds and is activated on the Au_n/TiO_2 surface.

II. EXPERIMENTAL DETAILS

The experiments were carried out in an ultra high vacuum (UHV) chamber with a base pressure of $<2\times10^{-10}$ Torr, attached to a size-selected cluster ion beam

[a)]Author to whom correspondence should be addressed. Electronic mail: anderson@chem.utah.edu

deposition system, described in previous publications.[15–17] In addition to the deposition system, the main chamber contains facilities for x-ray photoelectron spectroscopy (XPS), Auger electron spectroscopy (AES), low energy ion scattering spectroscopy (ISS), and mass spectrometry. The XPS experiments used the Mg Kα (1253.6 eV) line from a dual anode x-ray source together with a hemispherical energy analyzer (Physical Electronics). The XPS binding energy scale was calibrated using the oxygen and titanium peaks from the TiO_2 substrate, ultimately checked against the Au 4f XPS from gold foil.

The model catalysts for these experiments were prepared by Au_n^+ deposition on a rutile $TiO_2(110)$ crystal ($7\times5\times1$ mm, Commercial Crystal Laboratories), mounted on a molybdenum backing plate (0.2 mm thick) to ensure even heating and cooling. The temperature of the crystal can be varied using either resistive or electron bombardment heating in conjunction with liquid nitrogen cooling. Most of the present experiments were done with the sample at room temperature throughout. Sample temperatures were measured by a K-type thermocouple attached to the edge of the TiO_2 crystal with UHV compatible ceramic cement (Aremco, Ceramabond 571). The $TiO_2(110)$ single crystal was cleaned by repeated cycles of Ar^+ bombardment and annealing at 1100 K in vacuum. This treatment also creates bulk oxygen vacancies, making the sample conductive enough for ion deposition and electron/ion spectroscopies with minimal charging. During the experiments, the cleanliness of the sample was frequently checked by XPS and ISS. Before each gold cluster deposition experiment, previously deposited gold and other contaminants were removed by 1 keV Ar^+ sputtering, then the TiO_2 was annealed for 15 minutes at 850 K in UHV. This treatment leaves a near-stoichiometric TiO_2 surface, however, both Ti XPS and water temperature-programmed desorption (TPD) (Ref. 18) indicate 7–10 % oxygen vacancy concentration.

Gold was deposited as Au_n^+ on room temperature TiO_2, in a 2 mm spot determined by an exposure mask positioned just in front of the sample surface. The spot was occasionally profiled by XPS or AES, and is homogeneous within the experimental resolution ($\sim80\ \mu$). The gold dose was monitored continuously during deposition by computer integrating the Au_n^+ current on the sample. The Au_n^+ beam was generated by laser vaporization of gold into a helium flow, which then expands into vacuum. Ions are collected by a series of radio-frequency quadrupoles that mass select the clusters and guide the beam through eight differential pumping walls into the UHV chamber. The kinetic energy spread of the Au_n^+ beam is less than 1 eV, measured by retarding potential analysis on the target, and for these experiments the clusters were deposited at an energy of 1 eV/atom. The gold coverage was fixed at 1.39×10^{14} Au atoms/cm^2, corresponding to 10% of a close-packed gold monolayer, except for Au_7, where the density was 10 times smaller, reflecting the low intensity of this cluster in our beam source. We opted to use a lower deposition density in this case to avoid overly long deposition times (>1 hour) where sample contamination would become an issue. Some deposition experiments were also performed at a sample temperature of 110 K to check for possible agglomeration at room temperature, however, no differences in gold dispersion are seen by ISS. The sintering behavior of gold deposited as Au^+ on TiO_2 has been examined in detail in a recent publication.[16]

To study the CO oxidation reaction, we used a pulse dosing technique similar to that recently described by Judai *et al.*[19] In this case, because the O_2 sticking probability is very low, the Au_n/TiO_2 sample was pre-exposed at room temperature to 600 L of $^{18}O_2$, to create a population of active surface oxygen species. The O_2 was then shut off, and the sample was exposed to the $C^{16}O$ reactant in the form of a series of 100 short pulses, with repetition rate of $\sim$0.066 Hz. Pulses were generated by a General Valve pulsed valve, driven by home-built electronics, and the CO was directed toward the surface by a dosing tube, to localize the CO pressure near the surface. The tube results in a delivered pulse that is asymmetrically broadened, with full width at half-maximum (FWHM) of $\sim$150 milliseconds (see below). Signals for $C^{16}O$ scattering from the surface, as well as for $C^{18}O$ and $C^{16}O^{18}O$, were measured with a differentially pumped (60 ℓ/s ion pump) mass spectrometer. The mass spectrometer views the sample through a 3 mm diameter orifice at the tip of the differential pumping cone, and the sample is positioned $\sim$2 mm from the aperture to allow CO reactants from the dosing tube to reach the surface. (O_2 pre-exposure is done with the sample retracted far from the aperture.) The CO backing pressure was adjusted to give an exposure of $\sim$0.2 L (0.05 ML) *per* pulse, as calibrated by measuring CO TPD from a Ni (100) crystal, in the same geometry. The sample-orifice-ionizer geometry used results in maximum sensitivity for species desorbing from the cluster-containing spot, with substantially lower sensitivity for species desorbing from surrounding regions of the TiO_2 crystal (see below).

III. RESULTS AND DISCUSSION

Previously, we reported CO oxidation activity for samples prepared by Au_n^+ ($n=1-4$, 7) on TiO_2. We will first summarize the size dependence, including new results for Au_5 and Au_6, then present a XPS and ISS results aimed at unraveling the origins of the strong size dependence observed, and finally an analysis of the temporal behavior of the samples.

A. The size dependence of CO oxidation activity

Figure 1 shows the raw data for $C^{18}O^{16}O$ desorbing from a sample prepared by Au_3^+ deposition, dosed with 600 L of $^{18}O_2$, then exposed to 100 $C^{16}O$ pulses of $\sim$0.2 L/pulse intensity (L=Langmuir=10^{-6} Torr sec). Several points should be noted. The CO_2 signal drops, roughly exponentially during the pulse sequence, reaching half the initial intensity after $\sim$24 pulses, corresponding to 4.8 L or $\sim$1.2 ML worth of impinging CO. The fluctuations in the CO_2 decay simply reflect the fact that our pulse doser has significant shot-to-shot intensity fluctuations when operating as required to deliver the small reactant pulses. These intensity fluctuations are also responsible for the apparent rapid drop in CO_2 intensity for the first few pulses—this behavior is not reproducible.

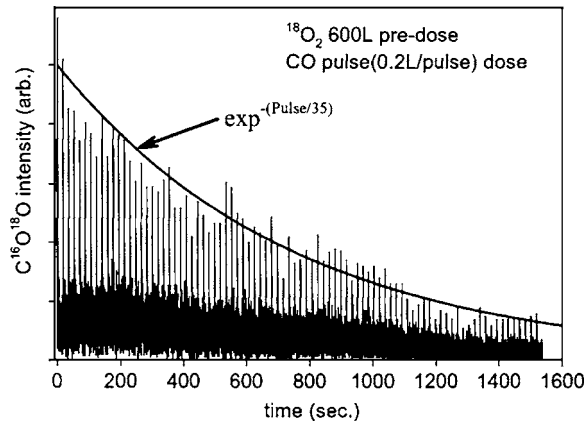

FIG. 1. CO_2 evolution during a sequence of 100 CO pulses of ~0.2 L/pulse intensity.

Note that if the sample is re-dosed with 600 L of O_2 following the sequence of 100 CO pulses, a second set of CO pulses results in CO_2 production 70–80 % of that observed in the initial experiment, suggesting that depletion of the oxygen reactant is mainly responsible for the decay in CO_2 production, and that O_2 exposure and CO oxidation does not strongly modify the samples at room temperature, at least for modest exposures.

Figure 2 compares CO_2 production from four different samples, showing only the first of the sequence of 100 CO pulses. The intensity scale for the CO_2 signal from all four samples is identical. For reference, the CO pulse is also plotted, divided by 100 to fit on the same intensity scale. Note that there is some CO_2 oxidation even on clean TiO_2, attributed to the presence of reactive oxygen species created on the TiO_2 surface by the 600 L $^{18}O_2$ exposure. Comparison of XPS for freshly annealed and O_2-exposed TiO_2 shows an O_2-induced decrease in the signal associated with Ti atoms at surface oxygen vacancies, indicating that O_2 is interacting with the vacancies. The nature of the oxygen binding is discussed further below.

The CO→$C^{16}O^{18}O$ conversion probability for TiO_2 is only ~0.3%, even for the first CO pulse, where the reactive oxygen concentration is at a maximum. The efficiency is low despite the fact that CO has a significant residence time and diffusion length on room temperature $TiO_2(110)$,[20] increasing the probability that impinging CO will encounter reactive oxygen. Low reactivity is consistent with the fact that it takes ~85 CO pulses (~17 L) to reduce the initial CO_2 intensity by a factor of e, indicating that the oxygen reactant is not very reactive, on average. Note, however, that more detailed consideration of changes in CO_2 pulse shape during the CO pulse sequence (below), suggests that there are at least two types of reactive surface oxygen species, one of which is highly reactive.

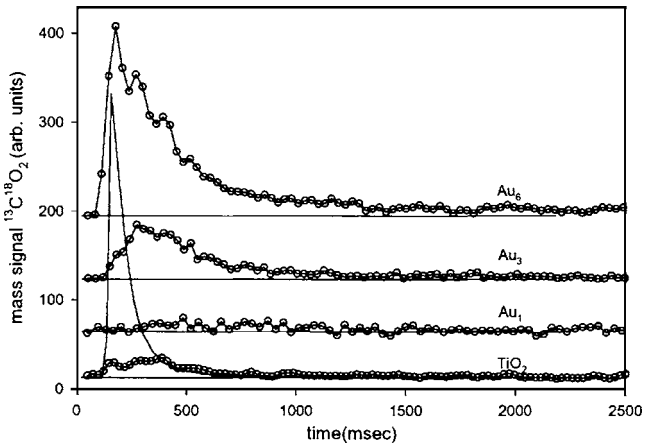

FIG. 2. Comparison of the CO_2 signal from the first CO pulse on O_2-pre-dosed TiO_2 and Au_n/TiO_2.

For the sample prepared by Au^+ deposition, there is almost no CO oxidation activity, i.e., there is no activity on the gold, and the activity that would result from O_2 interacting at vacancies is suppressed. This result is consistent with XPS results[16] showing that Au^+ diffuses to, and binds at vacancy sites on TiO_2 at room temperature. Evidently gold atoms poison the vacancies with respect to O_2 adsorption/activation. The fact that the CO_2 signal for Au^+/TiO_2 is much smaller than that for TiO_2 is consistent with the fact that the number of gold atoms deposited is more than enough to block all the vacancies. The very low CO_2 signal observed for the Au^+/TiO_2 sample also provides an upper limit on the background level of CO_2 that might be forming on surfaces such as the hot mass spectrometer filament. In short, this background is small compared to the CO_2 production on clean TiO_2, and negligible compared to the activity on samples prepared with Au_n^+, $n \geqslant 3$.

There are several possible sources for the small, but nonzero CO_2 signal observed for the Au_1/TiO_2 sample. There might be some gold agglomeration into catalytically active cluster sizes, however, the observation that the signal for Au_1^+/TiO_2 is so much smaller than for samples prepared with Au_n^+ ($n \geqslant 3$), indicates that agglomeration is not a serious problem. In addition, our mass spectrometer geometry allows some CO_2 from the TiO_2 immediately surrounding the deposition spot to enter the differential pumping orifice. The fact that the activity for Au/TiO_2 is much smaller than for TiO_2 indicates strong discrimination against this background signal, probably because additional collimation is provided by the ionizer/quadrupole entrance orifice.

For samples prepared by Au_2^+ deposition, there is a small increase in CO_2 production relative to the Au/TiO_2 sample, although the activity is still less than half that for clean TiO_2. The recent STM results of Buratto *et al.*[21] suggest that for deposition under conditions similar to ours, small gold clusters diffuse and bind intact at vacancy sites. The implication is that Au_2 bound at vacancies also poisons CO oxidation activity. The increased CO oxidation activity probably reflects the fact that the Au_2^+ deposition density is half the Au^+ density, increasing the probability that some vacancy sites are left gold-free to mediate the reaction.

For the sample prepared by Au_3^+ deposition, the CO_2 production level is well above the level seen for clean TiO_2, i.e., the gold species formed by Au_3^+ deposition have substantial CO oxidation activity. The activity for samples prepared by deposition of Au_4^+ and Au_5^+ is lower, although still above the activity originating from the support vacancies (an in-

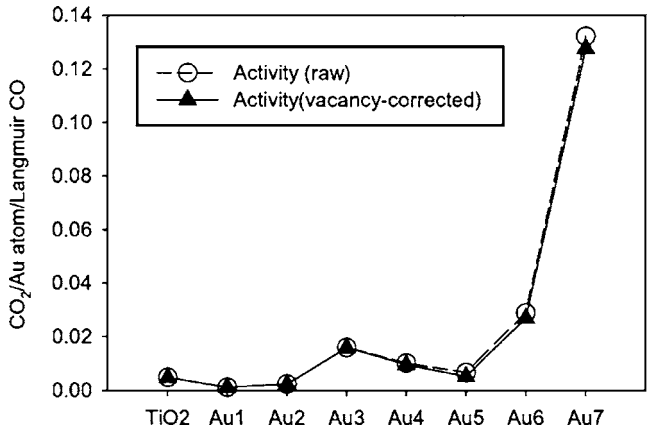

FIG. 3. Comparison of the CO oxidation activity for Au_n/TiO_2.

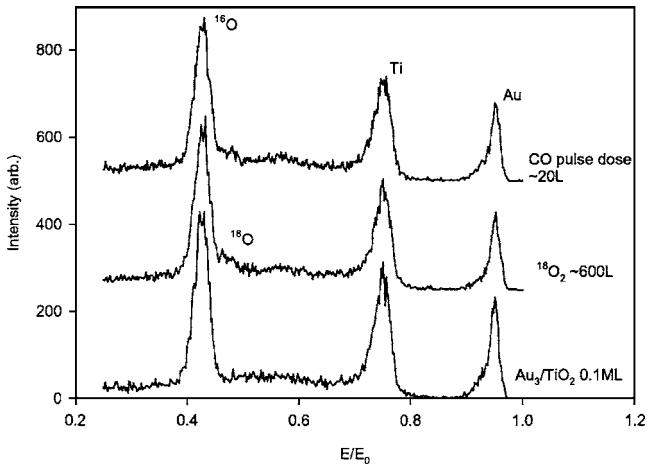

FIG. 4. (Bottom) ISS for as-deposited Au_3/TiO_2. (Middle) ISS after exposure to 600 L of $^{18}O_2$. (Top) ISS after 600 L O_2 exposure followed by 20 L exposure to CO pulses.

creasing fraction of which are vacant as the cluster size increases). As shown in the figure, however, the activity jumps substantially for Au_6^+ deposition.

Figure 3 shows the cluster size dependence of the activity, both raw and corrected for reaction at vacancy sites on the TiO_2. The activity scale is in units of $C^{16}O^{18}O$ molecules generated *per* L of incident $C^{16}O$, *per* deposited Au atom, thus accounting for lower Au density used for Au_7, compared to the other samples. The activity values were calculated from the integrated CO and CO_2 peak intensities, corrected for the relative ionization efficiencies of CO_2 and CO. The CO pulse intensity was calibrated by characterizing desorption of pulse-dosed CO from Ni(100). The intensities were averaged over the first four CO pulses, to reduce effects of shot-to-shot CO intensity fluctuations. For the sake of putting TiO_2 on the same scale, its CO_2/CO intensity ratio was normalized as if this sample had a reactive site concentration equal to the Au deposition density for Au_n/TiO_2 $(n=1-6)$. The vacancy correction was made assuming that the clusters deposit intact at vacancies (as suggested by the STM results of Buratto *et al.*,[21] and that activity at unoccupied vacancies on Au_n/TiO_2 is identical to that for clean TiO_2. The relative uncertainty in comparing different cluster sizes is estimated to be about 20%, and the absolute uncertainty is estimated to be about a factor of 3. The main sources of absolute uncertainty are the overlap of the mass spectrometer collection area with the cluster-containing spot, the exposure-*per*-pulse calibration, and possible variations in mass spectrometer transmission with mass.

We worried that the activity scale might be skewed by different collection efficiencies for CO_2, which is mainly produced in the deposition spot, and CO, which might scatter into the mass spectrometer from areas of the sample outside the spot, and/or be attenuated by reaction inside the spot. Therefore, the CO_2/CO intensity calibration was also checked by measuring ion signals for CO and CO_2 gas backfilled into the chamber over a range of pressures. The activity calibration obtained this way is within a few percent of that calculated as above, consistent with the conclusions (above) that the mass spectrometer is mainly sensitive to molecules desorbing from the spot, and that the CO reaction probability is quite small.

B. Sample morphology

The observation of sharp and nonmonotonic dependence of activity on deposited cluster size is evidence that the clusters remain approximately intact after deposition. This result does not exclude some fragmentation or agglomeration of the deposited gold, but if fragmentation or agglomeration were facile, it would wipe out the observed size dependence. In particular, deposited Au^+ and Au_2^+ clearly do not agglomerate into the reactive size range $(Au_n,\ n \geqslant 3)$ to a significant extent.

Morphology can also be probed in our experiment by ISS. Figure 4 shows typical raw ISS spectra for as-deposited Au_3/TiO_2, for Au_3/TiO_2 exposed to 600 L of $^{18}O_2$, and for the O_2-dosed sample after exposure to 100 CO pulses, as described above. For fixed scattering geometry, the peak positions (labeled ^{16}O, Ti, and Au) depend only on the masses of the surface atoms from which He^+ is scattered. Peak intensities depend on scattering cross sections, and on factors relating to shadowing, blocking, and ion survival probability (ISP).[22] The combined effect is to make He^+ ISS sensitive only to atoms in the top-most sample layer, and therefore sensitive to Au morphology and the presence of adsorbates.

Because the ISPs and shadowing/blocking effects for different atoms in various binding sites are unknown, absolute ISS intensities are difficult to interpret, however, changes in intensities can be related to changes in sample morphology. For reference, Fig. 5 shows the surface structure of rutile $TiO_2(110)$. From the perspective of ISS probing, several features are important. Oxygen exists both in terrace sites and in bridging oxygen rows, with 7–10 % vacancies among the bridging oxygen. The Ti atoms under the bridging oxygen rows are effectively second-layer atoms and are expected to contribute little to the Ti ISS signal, except where they are partially exposed by oxygen vacancies.

To correct for run-to-run fluctuations in the He^+ beam intensity, we analyze the ISS results as ratios of intensities for scattering from different types of atoms. The top trace in Fig. 6 shows the O/Ti ratio, normalized to the value for freshly prepared TiO_2. Note that for all the gold-containing samples, the O/Ti ratio is slightly greater than for clean

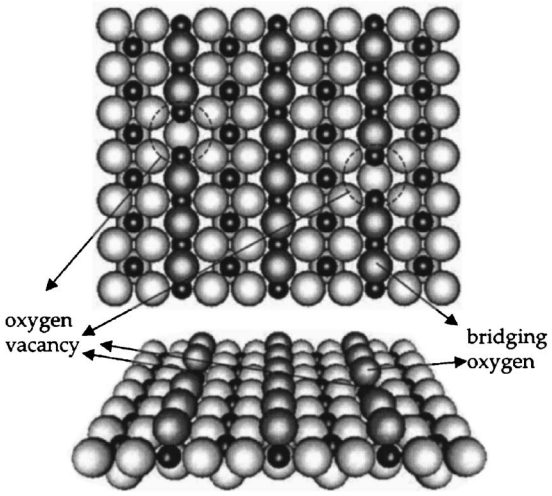

FIG. 5. The rutile $TiO_2(110)$ surface, in top and perspective views. Small black balls are titanium atoms, dark gray balls are bridging oxygen atoms, and light gray balls are oxygen atoms. Two oxygen vacancies are shown, circled in the top view.

TiO_2, i.e., deposited gold attenuates ISS from Ti more than from O. It is likely that this effect results from a propensity for Au to bind at oxygen vacancies, attenuating scattering from Ti atoms that would otherwise be exposed by the missing O. This conclusion is also supported by the observation that the Ti XPS signal associated with the vacancies is decreased upon gold deposition. It is interesting to note that for Ni_n/TiO_2[15] and Ir_n/TiO_2[23], the O/Ti ratios *decrease* after metal deposition, attributed to a propensity for metal binding on oxygen sites.

The gold morphology is more sensitively probed by the Au/substrate ratios, i.e., the ratio of the Au intensity to the sum of the O and Ti intensities. This ratio depends primarily on the fraction of the gold in the ISS-visible top layer, and to a lesser extent, on the degree to which the gold attenuates scattering from Ti and O atoms beneath and immediately surrounding the adsorption site (the attenuation "footprint"). The ratio should be at a maximum for gold ad-atoms dispersed on the TiO_2, because all Au atoms are accessible to the He^+ beam, and the attenuation of Ti and O signal is also maximized. Clustering of Au into 1-d or 2-d islands should result in a small reduction in the Au/substrate ratio for two reasons. The Ti and O signals increase slightly because the footprints of clustered Au atoms overlap, i.e., more of the surface is gold-free. In addition, although all Au is still in the top layer, intra-cluster shadowing and ISP effects result in a small decrease in Au signal. For low gold coverages, both effects are small. Large reductions in the Au/substrate ratio can occur only if some fraction of the gold is no longer in the top-most layer, i.e., if the gold is in multilayer clusters. Large decreases would also occur if gold becomes adsorbate covered, desorbs, or diffuses below the TiO_2 surface. Desorption (i.e., nonunit Au sticking probability) can be excluded as an explanation for the ISS dependence on cluster size, based on XPS results discussed next. The effects of adsorbates are demonstrated below. Diffusion subsurface does not appear to be an issue in this system, but its effects can be seen in ISS studies of Ir_n/TiO_2[23], and of Pt/TiO_2.[24]

Figure 6 also shows the Au/substrate ratio for samples prepared by Au_n^+ $(n=1-6)$ deposition. Data are not shown for Au_7^+, because this sample used a lower Au coverage, and cannot be directly compared. Also shown for comparison is the CO oxidation activity. As expected from the discussion above, the maximum Au/substrate ISS ratio is seen for the sample prepared with Au^+ deposition. This does not prove that the sample consists of dispersed atoms, but does show that the average dispersion is larger than in any of the samples prepared by cluster deposition. For Au_2^+ through Au_4^+, the Au/substrate ratio is reduced about 10%, and roughly constant. We propose that these samples consist mostly of small 1-d or 2-d (i.e., single layer) gold clusters, as would occur if the clusters remained intact upon deposition. For Au_5 and Au_6, the Au/substrate ratio begins to decrease significantly, and we propose that the change signals the onset of a transition to 3-d clusters. Even a single Au atom on top of an otherwise planar structure would substantially attenuate scattering from the underlying gold, and the modest decreases in Au/substrate ratio may simply indicate an increasing fraction of 3-d clusters. Given that we have no control over impact orientation, it would not be surprising if there were some distribution of deposited cluster shapes, particularly if there is a significant activation energy for 3-d $\Leftrightarrow$ 2-d diffusion.

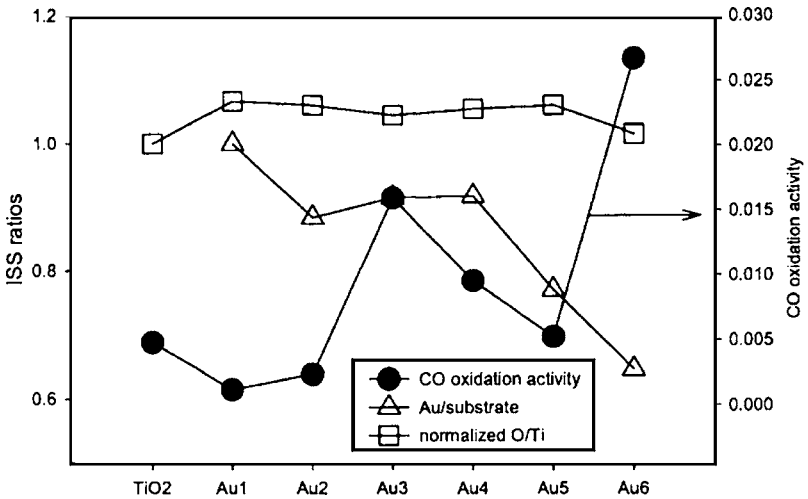

FIG. 6. Comparison of ISS ratios for as-deposited Au_n/TiO_2 (left scale) to CO oxidation activity (right scale).

For comparison, Fig. 6 also shows the CO-oxidation activity vs cluster size. Activity generally rises as the Au/substrate ratio decreases, however, the correlation is not one-to-one, suggesting that some factor other than cluster morphology controls activity in this size range. Goodman and co-workers have reported several studies, both for Au nanoparticles (2–3 nm diameter) on TiO_2,[7] and for Au layers grown on TiO_x/Mo(112),[25] suggesting that two layer thick gold is particularly active. In our experiment, Au_5 appears to be the first size which has a significant fraction of 3-d (i.e., two layer) clusters, yet this is a particularly unreactive size. While the increasing activity for Au_6 and Au_7 suggests that cluster thickness may be important, it is perhaps not surprising that other factors are also important for our very small clusters.

Before examining these factors, it is useful to compare the interpretation of our ISS results with the STM results of Buratto *et al.*[21] They conclude from height measurements that Au_2-Au_4 are single layer clusters, consistent with our results. For Au_5-Au_7, they observe average heights consistent with two layer clusters, and our results also indicate a transition to two layer clusters, although the ISS results are more suggestive of an increasing fraction of two layer clusters. The only serious discrepancy is that they observe large sintered clusters when depositing Au^+. This result is clearly inconsistent with our high Au/substrate ISS ratio for Au/TiO_2, with our measured CO-oxidation size dependence, and with XPS results,[16] which all rule out substantial sintering. It is not clear what causes the difference between the two experiments. The $TiO_2(110)$ surface is prepared similarly, and deposition is under similar conditions. The major difference may be experimental time scales. For atoms, our typical time between starting deposition and either ISS or CO-oxidation analysis is 10–15 minutes, compared to ~2 hours for the STM experiments.[21] We do observe that samples allowed to stand in our vacuum system overnight behave differently than fresh samples, although we cannot say whether this results from sintering or contamination.

For the case of Au^+/TiO_2, we recently reported a study of the annealing behavior for T_{anneal} between 100 and 800 K.[16] The conclusion was that deposited gold atoms do diffuse at temperatures between 200 and 300 K, but they mostly become trapped at oxygen vacancy sites. Significant agglomeration on a 5 minute timescale was observed only for T_{anneal} above room temperature. Thermal agglomeration can also be inferred from its effects on CO oxidation activity, as shown in Fig. 7. This figure shows room temperature CO_2 production under conditions identical to those in Fig. 1, for a sample prepared by Au^+ deposition, but annealed to different temperatures for 5 minutes before reactant exposure. The vertical scale has been decreased by a factor of 7 compared to that in Fig. 1, allowing the small activity for the unannealed Au/TiO_2 sample to be seen more clearly. 400 K annealing substantially increases the activity, and the increase continues up to $T_{anneal}=600$ K, presumably indicating the presence of a distribution of active clusters. XPS after annealing to $T_{anneal} \geq 450$ K shows that ~70% of the gold has near-bulk 4f binding energies, i.e., is in the form of clusters. Note, however, that the peak activity never exceeds that of the sample prepared by Au_3^+ deposition, and activity decreases for $T_{anneal}=700$ K. Given that Fig. 3 suggests a strong increase in activity with cluster size, it is unclear why the annealed samples are not more active. If the gold were agglomerated into large multilayer particles, low activity might result simply because the exposed gold surface area would be reduced. This scenario is excluded by ISS measurements indicating that more than half the gold atoms are still in the top sample layer even after 800 K annealing.[16]

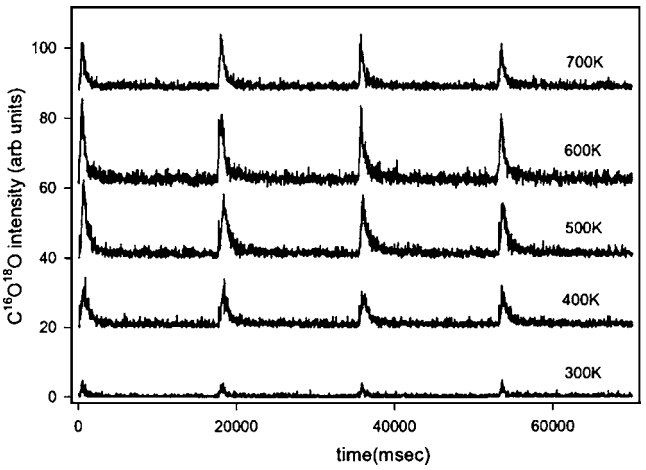

FIG. 7. Effects on CO_2 production of annealing an Au_1/TiO_2 sample to the indicated temperatures prior to O_2 exposure and CO pulsing.

C. XPS characterization

One factor that might reasonably be expected to result in size-dependent CO oxidation activity is changes in gold electronic structure with cluster size. Our only probe of gold electronic properties is the Au 4f XPS, which was measured after room temperature deposition for Au_n^+ $(n=1-6)$ on TiO_2. Within experimental error, the Au intensity is independent of cluster size, indicating that sticking probability is also size-independent, and presumably near unity. In addition, the peak position, 84.7 eV compared to 84.0 eV for bulk gold, is also size-independent within our resolution.

Chusuei *et al.*[26] reported a set of Au 4f binding energy measurements for various coverages of Au on $TiO_2(110)$, and also characterized the corresponding cluster size distributions by STM. Their paper has a nice discussion of the origins of binding energy shifts. For low Au coverages in the range used in our experiments, their data show a shift of ~0.8 eV relative to the bulk limit—within experimental error of the ~0.7 eV shift we observe. The absence of a dependence on cluster size in our results is somewhat surprising, because the trend observed by Chusuei *et al.* for binding energy vs gold coverage suggests that there should be an increase in binding energy as cluster size decreases. Such shifts are attributed to decreasing final state screening as metal aggregate size is reduced. Indeed, we observe just such an increase in deposition of size-selected gold clusters on alumina.[27]

For TiO_2, however, the XPS interpretation is complicated by the presence of a large concentration of surface oxygen vacancies, which tend to act as binding sites for gold.

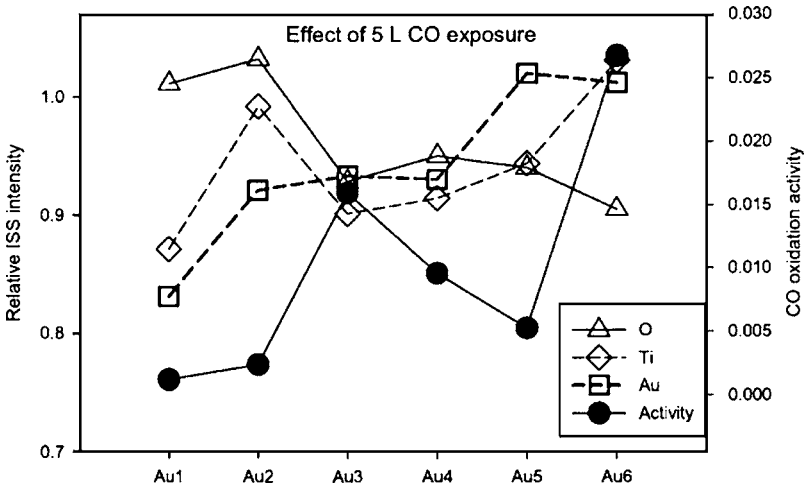

FIG. 8. Effects of 5 L CO exposure on the intensity of ISS peaks for O, Ti, and Au, relative to their pre-exposure intensities (left scale). Also shown (right scale) is the CO oxidation activity.

Because extra electrons are associated with these vacancies and gold is quite electronegative, binding at vacancies tends to inject electron density into the gold.[16,28] This increased electron density results in an initial state shift, decreasing the XPS binding energy. We speculate that the approximate constant binding energy for these small clusters results from the combination of these two offsetting effects. Final state effects should tend to increase XPS binding energy as cluster size decreases. The electron density injected into the gold from the vacancy must be more localized for smaller clusters, however, tending to decrease XPS binding energy. As noted above, if the Au/TiO_2 samples are annealed at high temperatures, the XPS does shift to near the bulk binding energy.[27]

XPS was also used to examine the Au_n/TiO_2 samples after exposure to the 600 L O_2 pre-dose, and after interaction with the series of CO pulses (totaling ~20 L), and little change was observed. Because the Au XPS is insensitive to deposited size and adsorbate exposure, we have to look elsewhere for insight into the size dependence of the CO oxidation reaction.

D. ISS characterization of adsorbate binding

Another potential factor influencing CO oxidation activity is binding of CO to the samples. Figure 8 shows the effect of 5 L CO exposure (~1.3 CO impinging/surface atom) on the ISS intensities for O, Ti and Au, relative to the intensities measured before the CO exposure. For this experiment, the samples did not receive the 600 L O_2 pre-exposure. It is important to recognize that for an effect to be seen by ISS, adsorption must be stable on the ISS timescale. The actual ISS scan time is about one minute, but up to 5 minutes can elapse between the adsorbate exposure, and completion of the ISS run. Therefore, to be seen in ISS, adsorbates have to be bound by ~0.9 eV (assuming an Arrhenius pre-factor of 10^{13} for desorption).

For Au_1, the gold signal is attenuated ~17% by CO exposure, indicating that a significant fraction of the gold sites have CO adsorbed in such a way as to attenuate scattering from gold. For Au_2, Au_3, and Au_4, the attenuation is about half that found for Au_1, and CO causes no attenuation for Au_5 and Au_6. The attenuation to be expected from adsorbed CO depends strongly on the adsorption geometry. For Ir_n/TiO_2, for example,[23] CO adsorbed atop iridium results in a large Ir ISS attenuation (~70% from 5 L CO), however, CO was also found to adsorb on the TiO_2 support around the periphery of the Ir clusters, and in that case there is little attenuation of ISS signal from Ir. The lack of Au ISS attenuation observed for CO exposure on Au_n/TiO_2 ($n=5$, 6) could, therefore, result from an absence of CO adsorption on the ISS timescale, or from CO adsorbed in peripheral sites. In the case of $CO/Ir/TiO_2$, the peripheral CO was clearly observed by CO TPD, but no obvious desorption peak is observed for Au_n/TiO_2. This result suggests that the CO coverage on Au_5 and Au_6 is not large, however, our sensitivity might be too low to observe a small amount of CO, particularly if the desorption feature is broad, as might occur if there were substantial restructuring of the samples during TPD. We are not aware of any studies of CO adsorption for very small gold clusters on titania for comparison. DFT calculations suggest that CO binds atop gold for isolated gold atoms, but for large gold "bars" on the surface, CO binds to the side of the gold, where it would not cause much ISS attenuation.[28]

The effect of CO exposure on the O and Ti signals is interesting as well. First, it should be noted that there is no ISS signal for carbon, indicating that any adsorbed CO is in the carbon-down orientation, and there is no dissociative adsorption that leaves carbon atoms in the top layer. As the cluster size increases, the CO attenuation of Ti signal gradually disappears, approximately in parallel with the decreasing affinity of Au_n for CO. Ti attenuation might result from either CO bound on the support, or CO bound atop gold shadowing an area on the TiO_2 support. The fact that both Au and Ti signals for Au_5 and Au_6 show little attenuation from CO exposure, suggests that there really is little CO bound.

The effects of CO on the O ISS signal are more complicated. For Au_1 and Au_2, there is no attenuation of O signal by CO (actually a slight increase), despite the fact that there is clearly CO adsorption atop gold, and such CO presumably shadows substrate O centers. This seemingly contradictory result can be rationalized by recognizing that CO bound on gold presents "extra" O atoms to the ISS beam, thus compensating for shadowing of substrate O. For Au_3 and larger

clusters, however, there is a small, but reproducible CO-induced attenuation of O ISS, which is surprising because the Au and Ti ISS results suggest that there is little CO binding for these larger clusters. Note that CO-induced O attenuation starts with Au_3, i.e., it occurs only for Au_n that are active for CO oxidation. This correlation raises the possibility that both the CO-induced O attenuation, and the absence of CO-induced Au and Ti attenuations, might result from gold-catalyzed reaction of CO with surface oxygen. The problem with this scenario is that it is unclear where the reactive oxygen would come from, because oxygen in the TiO_2 lattice is not reactive under our conditions (see below).

The figure also shows the CO oxidation activity. The trends in activity and CO-exposure effects on Au ISS are grossly similar (i.e., activity is anticorrelated with CO attenuation of Au signal), however, there is no cluster-by-cluster correlation, suggesting that the ability of the clusters to bind CO (such that Au ISS is attenuated) is not the limiting factor in CO oxidation activity under our conditions.

Comparison of the lower two traces in Fig. 4 shows the effects of 600 L $^{18}O_2$ exposure on the ISS spectrum for a typical sample. All three original peaks (^{16}O, Ti, Au) are attenuated and a new shoulder for scattering from ^{18}O appears. For clean TiO_2, the Ti and ^{16}O attenuations are ~20% and ~11%, respectively, and the resulting ^{18}O peak has intensity ~10% of that for ^{16}O. These changes indicate that ^{18}O is left on the surface, and binds in such a way as to reduce He^+ scattering from both ^{16}O and Ti. The larger effect on Ti is expected, because ^{18}O will bind preferentially at vacancies, and vacancy sites contribute a disproportionate fraction of the Ti signal, as discussed above. The changes in ^{16}O and ^{18}O signals could, in principle, result either from ^{18}O replacing ^{16}O in the surface layer, or from ^{18}O adsorbing (as O or O_2) on top of the surface layer, blocking scattering from the underlying ^{16}O. The substantial decrease in Ti signal indicates that there is net addition of O to the surface, rather than simply exchange of ^{18}O for ^{16}O.

These results can be compared to the literature on O_2 interaction with TiO_2. Temperature dependent adsorption/desorption studies suggested a dissociative adsorption mechanism for O_2/TiO_2 (Refs. 18 and 29) and Pan *et al.*[30] showed additional evidence for dissociative adsorption with ISS. A recent STM study by Schaub *et al.*[31] showed that oxygen molecules bind and dissociate on the oxygen vacancy sites, generating atomic oxygen. DFT calculations[28,32] indicate the possibility of several types of O and O_2 binding arrangements in association with vacancies.

Similar $^{18}O_2$-induced ISS peak attenuations are observed for Au_n/TiO_2 samples, as summarized in Fig. 9. The attenuations of ^{16}O intensities are less that ~10% for all samples, presumably reflecting a combination of ^{18}O exchanging with substrate ^{16}O, binding atop the TiO_2, and binding on gold such that some area of the substrate is shadowed. The attenuations of Ti and Au signals are larger, with stronger cluster size dependence. For Au_1 there is little attenuation of Au signal, indicating that there is not much O adsorption atop Au, and somewhat larger Ti attenuation indicating that there is additional O adsorbed on the support. For this sample, we expect that nearly all the vacancy sites are gold-occupied,

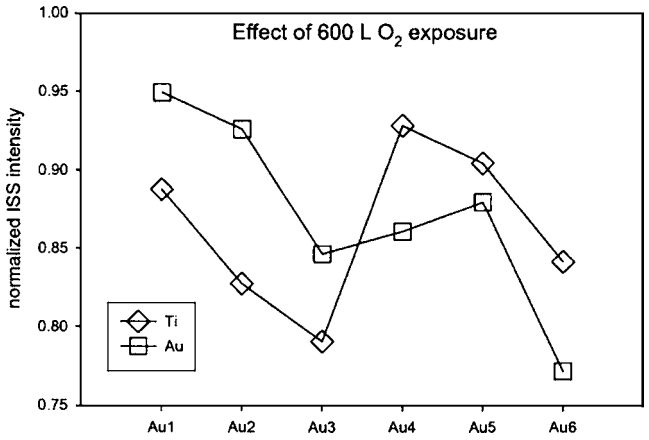

FIG. 9. Effects of 600 L $^{18}O_2$ exposure on the Ti and Au ISS intensities, relative to the pre-exposure intensities.

therefore it is not clear which Ti atoms are being affected by $^{18}O_2$ adsorption. There may be some oxygen adsorption on the substrate adjacent to gold, or possibly at substrate steps or other defects.

As cluster size increases to Au_3, the attenuation of Au signal increases, indicating that an increasing fraction of the gold has ^{18}O on top. Simultaneously, the lower cluster density leaves an increasing fraction of gold-free vacancies where $^{18}O_2$ can adsorb. Both effects probably contribute to the observed increase in $^{18}O_2$-induced Ti attenuation. For Au_4 and Au_5, the Au attenuations decrease, indicating that less O is adsorbed atop gold. Curiously, there is a large decrease in $^{18}O_2$-induced Ti attenuation, despite the expectation that there should be an increasing number of gold-free vacancies where oxygen adsorption should attenuate exposed Ti. It is not clear what might cause this apparent lack of adsorption at vacancies, unless the presence of Au clusters in this size range decreases the oxygen affinity of nearby vacancy sites. Such an effect would not be entirely surprising, as the presence of gold must have some effect on the substrate electronic structure. Finally, at Au_6 there is a large increase in O-induced attenuation of Au signal, indicating that a larger fraction of Au has O adsorbates. This increase is also accompanied by an increase in Ti attenuation, presumably from shadowing effects. For comparison, it is interesting that Bondzie *et al.*[6] observed ~50% attenuation of Au ISS for oxygen-dosed nanometer size gold particles on TiO_2, however, they dosed the surface with atomic oxygen, where the sticking coefficient is much greater.

The most interesting result is that there is an excellent anticorrelation between CO oxidation activity and the O_2-induced attenuation of Au ISS signal. As attenuation increases (i.e., as Au ISS intensity after O_2 exposure decreases), so does CO-oxidation activity. The correlation is good on a cluster-by-cluster basis, as shown in Fig. 10, which compares CO oxidation activity with the O_2-induced Au ISS attenuation, plotted on an inverted scale. It seems clear from the one-to-one correlation, that activity is controlled by the ability of the clusters to bind oxygen in such a way that Au ISS intensity is attenuated. ISS does not show whether this ISS-visible oxygen is molecular or atomic, or exactly how it binds to the gold, however, chemical intuition

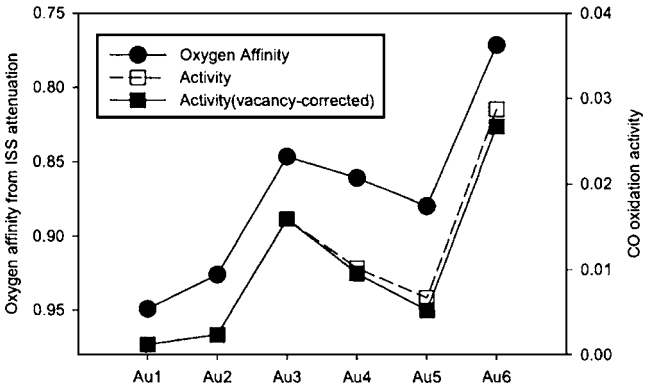

FIG. 10. Correlation of CO oxidation activity (right scale) with the O_2-induced attenuation of Au ISS signal (left scale, inverted).

suggests that it probably is atomic O bound atop the gold clusters. DFT calculations[28,33] show that for gold clusters bound at vacancy sites, O_2 can be adsorbed at the interface between TiO_2 and the gold cluster, with considerable destabilization of the O-O bond, allowing dissociation at room temperature. As discussed above, O_2 can also bind and dissociate at vacancies on the TiO_2 surface, however, the concentration of such substrate-bound oxygen is not directly correlated with activity. This issue is discussed further in the next section.

E. CO oxidation kinetics

CO oxidation activity is strongly correlated with the amount of ISS-visible oxygen bound to gold, but there is evidence from Ti ISS attenuation, and from activity on clean TiO_2, that oxygen also binds to other sites on the surface. The pulsed reaction experiments provide several additional pieces of information relating to the CO oxidation mechanism and its dependence on cluster size. It is interesting to look at the decay of CO_2 production during the sequence of 100 CO pulses (Fig. 1). The decays for all samples are roughly exponential: $I_n = I_1 \cdot \exp[-(n-1)/Q]$, where I_1 and I_n are the CO_2 intensities for the 1st and nth pulses, and Q is a constant characterizing the decay. As discussed above, the decay largely appears to be driven by depletion of the reactive oxygen concentration, as shown by recovery of CO_2 signal upon O_2 re-dosing of depleted samples.

We also considered the possibility that the decay was, instead, the result of poisoning of the active sites during the CO pulse sequence. For example, if CO bound strongly to the clusters or in support sites surrounding the clusters, it might block access to the active sites, or modify their chemical properties. This explanation for the CO_2 decay seems unlikely based on consideration of the relative amounts of CO and gold. A single 0.2 L CO pulse delivers $\sim 7.7 \times 10^{13}$ CO/cm^2, corresponding to between ~ 0.5 and ~ 4 CO molecules per cluster for Au_1 through Au_7. Therefore, no more than a few CO pulses would be required to occupy all the strongly bound sites, and if poisoning were an issue, the CO_2 intensity would decay much more rapidly than is observed. Furthermore, if this putative poisoning CO is unreactive with the reactive oxygen already present on the samples, it is unclear why the activity would be restored by re-exposure to molecular O_2. We cannot exclude buildup of strongly adsorbed CO, but if such CO exists it does not strongly affect the reactivity, nor does it produce obvious signatures in TPD or ISS.

Values of Q for all the samples are given in Table I, and vary from 35 for Au_3 to 85 for Au_5 and for clean TiO_2. Consider the Au_3/TiO_2 sample, where Q is 35, corresponding to 7 L of CO exposure, or ~ 1.7 CO molecules impinging from the gas phase *per* surface atom. If CO oxidation occurred only for CO impacting directly on an active surface O atom, as in an Eley–Rideal mechanism, the Q value would imply that the reaction efficiency *per* direct CO-O collision is ~ 0.58, i.e., $I/I_0 = e^{-1} = \exp(-1.7 \cdot 0.58)$. As shown by Bowker and co-workers, however, CO has a residence time of several hundred nanoseconds on room temperature $TiO_2(110)$,[20] during which time CO can diffuse and encounter clusters. The importance of this substrate-mediated adsorption effect for small, highly dispersed clusters is demonstrated by the observation that small Ir clusters deposited at 10% ML density on $TiO_2(110)$ collect essentially every CO molecule impinging on the sample, regardless of whether the

TABLE I. CO_2 production parameters.

Sample	Decay Q[a]	1st pulse CO_2 per Au atom	CO_2 per CO	CO_2/Au atom in 100 CO pulses	Total[b] CO_2 per Au atom	ISS-vis. O per Au atom	CO_2/O 100 pulses	Total[b] CO_2/O
TiO_2	85	9.56e-04[c]	1.73e-03	0.05[c]	0.08[c]		0.20[e]	0.28[e]
Au_1	80	2.37e-04	4.29e-04	0.01	0.02	0.05	0.27	0.37
Au_2	65	4.71e-04	8.54e-04	0.02	0.03	0.07	0.33	0.41
Au_3	35	3.19e-03	5.78e-03	0.11	0.11	0.15	0.69	0.72
Au_4	45	1.91e-03	3.47e-03	0.08	0.09	0.14	0.56	0.62
Au_5	85	1.05e-03	1.90e-03	0.06	0.09	0.12	0.51	0.74
Au_6	55	5.35e-03	9.70e-03	0.25	0.29	0.23	1.09	1.29
Au_7	43	2.55e-02	4.63e-02[d]	1.00	1.09			

[a]Decay constant Q: $I = I_0 \cdot \exp(-\text{pulse}/Q)$.
[b]Extrapolated total CO_2 production or complete active O depletion, assuming exponential decay.
[c]To allow comparison of TiO_2 results, the CO_2 production is normalized as if TiO_2 had an active site density equal to the Au density on the Au_n/TiO_2 samples (1.4×10^{14}/cm^2).
[d]Scaled by a factor of 10 to compensate for 10 times lower Au atomic density for the Au_7 sample.
[e]Calculated based on the assumption that the active O density is equal to the initial vacancy density.

initial adsorption is on Ir or on the surrounding TiO_2.[23] The 4th column of Table I shows the number of CO_2 molecules produced *per* CO incident on the sample (0.0058 for Au_3). These CO_2/CO values would be the reaction efficiencies if we assume that all impinging CO molecules encounter an active site during their lifetime on the surface.

It is clear that CO oxidation activity under our conditions is strongly correlated with the amount of oxygen bound on the gold clusters, such that it attenuates Au ISS. It is less clear, however, whether only this ISS-visible oxygen is reactive, or if oxygen initially bound on the support might diffuse to the active sites and react. The ^{16}O and Ti ISS results suggest that such support-bound oxygen exists, possibly bound at the periphery of the clusters or at vacancies and other support defects. The data provide two ways to address this question. Re-dosing experiments suggest that the Q values mainly reflect depletion of the reactive oxygen concentration by CO oxidation. In that case, the Q values should be inversely related to the CO oxidation activity for each sample, i.e., the reactive oxygen should be more rapidly depleted on more active samples.

The column labeled "1st pulse CO_2/Au atom" in Table I gives the number of CO_2 molecules produced *per* Au atom in the first CO pulse, i.e., this is a measure of the initial activity. Comparison of these values with the Q values in the table show that the expected inverse relation holds qualitatively, but not quantitatively. For example, the initial activity is ~1.7 times higher for Au_6 compared to Au_3, yet Au_6 also has the higher Q value. Of course, the other factor entering into the relation between activity and Q, is the initial concentration of the reactive oxygen, built up during the O_2 pre-exposure. The ISS results in Fig. 9 indicate that samples prepared with different cluster sizes do bind different amounts of oxygen, and in particular, the ISS-visible oxygen concentration is substantially larger for Au_6 than for Au_3. On the other hand, it is not clear that the increase in ISS-visible oxygen for Au_6 can account for the entire increase in CO_2 production, thus we need to consider the possibility that oxygen initially bound to the TiO_2 participates in the reaction.

We can address the question of whether substrate-bound oxygen is *required* in the mechanism by simply comparing the amount of ISS-visible oxygen to the total amount of CO_2 produced. To calculate the ISS-visible oxygen concentration, it is necessary to assume something about the Au attenuation *per* O atom, which depends on the nature of the O-Au binding. For our ISS geometry, with detection along the surface normal, an O atom bound directly atop a Au atom would completely block signal from the underlying Au atom. This is presumably the case for O bound to dispersed atoms. If O is bound in a bridge or hollow site on a gold cluster, then ISS signal from more atoms is attenuated, but the *per* atom attenuations are smaller. For the purposes of estimating the ISS-visible O concentration, we assume that this oxygen is adsorbed as atoms, and that each O atom attenuates one Au atom's worth of Au ISS signal on average. While this assumption is questionable, it should be adequate for comparison to the absolute CO_2 production levels, which are only known to a factor of ~3, as discussed above. The Au ISS attenuating range from 5% for Au/TiO_2 to 23% for Au_6/TiO_2 (Table I), so given the assumption above, this corresponds to O-on-gold concentrations between 5 and 23 % of the Au concentration. The total amount of CO_2 produced can be calculated by integrating the pulses of CO_2 desorbing during the sequence of 100 CO pulses. The result is given in the Table I column labeled "CO_2/Au atom in 100 CO pulses." Because activity, and therefore the fraction of reactive O removed in 100 pulses, varies considerably with cluster size, we also extrapolated the CO_2 production to the limit of complete reactive O depletion, using the exponential fit to the first 100 pulses ("Total CO_2 per Auatom"). Finally, the corresponding ratios of CO_2 production to initial ISS-visible O concentration are given as "CO_2/O 100 pulses," and "CO_2/O."

The important result of this bookkeeping analysis is that the amount of CO_2 produced is comparable to the initial concentration of ISS-visible O. In particular, the value of "Total CO_2/O" is unity within experimental error for the active cluster sizes Au_n, $n \geqslant 3$. This is just what is expected if only the initially ISS-visible oxygen reacts significantly—it all should be converted to CO_2 in the limit of infinite CO exposure. The fact that the ISS-visible oxygen is sufficient to account for all the CO_2 does not rule out participation by oxygen initially bound on the support, but suggests that diffusion of support-bound oxygen is probably not be a limiting factor in the mechanism.

The "Total CO_2/O" ratios for Au_1, Au_2, and for clean TiO_2 are substantially less than unity, but this observation is probably not mechanistically significant. The Au_1 and Au_2 samples are so unreactive that extrapolating to complete O depletion is highly uncertain. In the case of the clean TiO_2 surface, we have no ISS data to quantitate the reactive oxygen concentration, therefore the CO_2/O estimate was based on the assumption that interaction of O_2 with vacancies on the as-prepared TiO_2, leads to one active O *per* vacancy. The fact that the "total CO_2/O" ratio estimated this way is substantially less than unity simply tells us that the actual concentration of active ^{18}O (we detect $C^{18}O^{16}O$) is smaller than the initial vacancy density, possibly because some ^{18}O generated by O_2 dissociation at the vacancies recombine and desorb, or because ^{18}O exchanges with the predominantly ^{16}O surface.

One of the more interesting features of the pulsed reaction data in Fig. 2 is the temporal profile of the CO_2 pulses, and more particularly the dependence of the temporal behavior on cluster size. Figure 11 replots the first pulse data for clean TiO_2, and for Au_n/TiO_2 ($n=3, 5, 6$). To facilitate comparison, the data sets have been scaled and offset. The relative scale factors for TiO_2, Au_3, Au_5, and Au_6 are 10, 2, 4, and 1, respectively.

There are several points of interest. For all samples, CO_2 production occurs over the entire CO pulse, however, the CO_2/CO ratio is much higher during the long time tail of the CO pulse, than at the peak. This can be seen for the case of TiO_2 in the figure, where the CO pulse has been scaled to show that the long time decays of CO and CO_2 signal are coincident. This behaviour suggests that CO_2 production saturates in some fashion during the highest intensity portions of the CO pulse. It should be noted that while a single

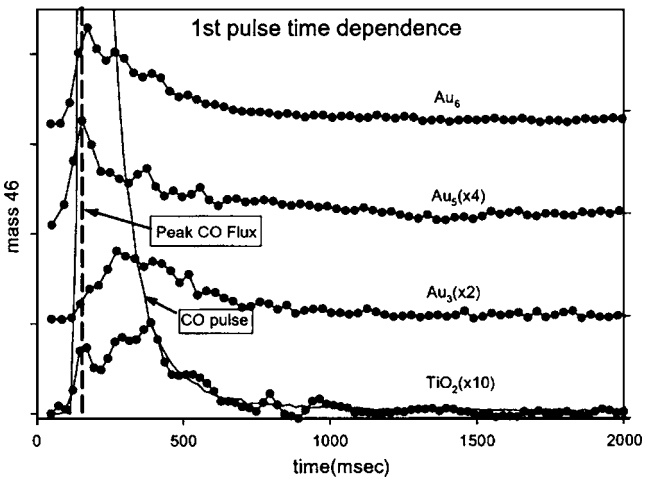

FIG. 11. Comparison of 1st pulse CO_2 pulse shapes for different cluster size samples.

pulse delivers only 0.2 L (~5% of a monolayer coverage), the peak CO flux is quite high, approximately equivalent to 10^{-6} Torr. Given that CO spends a few hundred nanoseconds diffusion on the surface,[20] it may be that several CO molecules are present at each active site during the peak flux, influencing the reactivity. For reference, it should be borne in mind that the average reaction probability *per* pulse is only ~1%, even for Au_6 (Table I).

Note that for TiO_2, there is a small CO_2 peak coincident with the CO peak (vertical dashed line), followed by a larger peak delayed by ~150 milliseconds. The early time, CO-coincident peak is reproducible, but it decays below the noise level in just a few CO pulses, whereas the main peak has a Q value of 85 pulses. The implication is that the $^{18}O_2$ exposed TiO_2 sample has two types of reactive oxygen sites. The minority site is highly reactive, resulting in a peak shape that tracks the CO pulse, and in complete depletion by just a few CO pulses. The majority site requires many Langmuirs of CO exposure to completely react away, and the inefficient reaction also apparently results in peak CO_2 production delayed with respect to the CO pulse. For this delayed pulse component, the pulse shape is unchanged over the 100 pulse sequence, within experimental error.

For Au_1 and Au_2, the CO_2 signal is too weak to allow meaningful analysis of the temporal behavior of individual pulses. For Au_5 and Au_6, the peak CO_2 production is coincident with the CO peak, although CO_2 peak/tail intensity ratio is much lower than the CO pulse. In contrast, for Au_3, Au_4, and Au_7, the peak CO_2 intensity occurs 100–200 msec after the peak CO flux. Both this time delay, and the fact that CO_2 production is less efficient during the CO peak flux, even for Au_5 and Au_6, must relate to the kinetics of reactant approach to the active site, reaction, and desorption of the CO_2 product. It is important to note that it is not possible to rationalize delayed CO_2 evolution solely in terms of slow kinetics for the actual CO oxidation event. There must also be a mechanism for storing either reactants or products on the surface on the hundred millisecond timescale. The point is best illustrated, perhaps, by outlining several conceivable mechanisms.

We start by noting that the correlation between activity and ISS-visible oxygen implies that the oxygen reactant is already present on the gold clusters at the start of the CO pulse. Furthermore, the total CO_2/O ratios discussed above indicate that only this gold-bound oxygen is required to account for the CO_2 production. Therefore, while diffusion of the oxygen from support to active sites cannot be excluded, this is not expected to play a significant role determining the temporal behavior of a single pulse. This conclusion is reinforced by the observation that the peak shapes do not change over the course of the 100 pulse sequence, even though the reactive oxygen concentration decreases substantially. CO diffusion is important, however, because most CO impinges on the support and must diffuse to the active site. Bowker has estimated[20] that CO has a lifetime of only a few hundred nanoseconds on the room temperature TiO_2 surface, thus CO diffusion can only affect the millisecond temporal profiles if the CO-TiO_2 binding energy is substantially enhanced in the vicinity of gold clusters.

If the CO_2 product had substantial (and cluster-size-dependent) binding energy to the samples, this would trivially account for the observed temporal behavior. The desorption energy of CO_2 on Au/TiO_2 has not been measured to our knowledge, and certainly not for the small clusters of interest here. There are data, however, suggesting that CO_2 desorption kinetics are unlikely to be in the 100 millisecond range at room temperature. Mullins and co-workers have found that CO_2 desorbs on the second timescale below 120 K from both Au(111) and oxygen-covered Au(111),[34] and have reported CO_2 evolution on the ~1 s timescale during pulsed CO oxidation on low coverage $Au/TiO_2(110)$ at 77 K.[3] If the CO_2 binding energies are comparable on our $Au_n/TiO_2(110)$ samples, then the desorption kinetics would be in the microsecond range. We attempted to measure CO_2 TPD from samples containing small Au_n, following CO_2 exposure at 140 K. No desorption features were observed in the temperature range above 140 K, consistent with expectations based on the Mullins results. It appears that CO_2 desorption kinetics do not significantly affect the CO_2 temporal dependence.

With these considerations in mind, several scenarios can be imagined that might result in 100 millisecond kinetics for CO_2 evolution.

(1) The CO-TiO_2 binding energy is large in association with the gold clusters, and the actual CO oxidation step is slow. We do not see much CO binding atop the gold clusters in ISS (Fig. 8), but this observation does not preclude strong binding on the support adjacent to the clusters. Slow kinetics for the oxidation step is consistent with the observation that only a small fraction of the incident CO is converted to CO_2. In this scenario, the CO_2 evolution temporal dependence is controlled by the CO oxidation kinetics, but the strong CO binding is also important because it provides a non-negligible probability that CO binds at the active site long enough for reaction to occur. In this scenario, the CO oxidation activity is determined by the convolution of the probability that CO will diffuse and bind to the clusters, the CO lifetime in association with the clusters, and the rate of the CO oxidation step. This combination of factors makes it possible to rationalize the observation that the most active clus-

ters do not necessarily have the fastest CO_2 evolution rates. For example, Au_7 and Au_3 show delayed CO_2 evolution, despite being more reactive than Au_5, where CO_2 evolution is prompt. Such behavior would result if CO binds more strongly to Au_3 and Au_7 than Au_5, such that the oxidation efficiency is higher, despite slow kinetics for the actual CO oxidation step. In this scenario, the observed "saturation" behavior might result if reaction were inhibited when more than one CO binds at the active site, or alternatively, if the binding energy for a second CO at an active site is so weak that it desorbs rather than reacting.

(2) CO binding to the TiO_2 is enhanced in the vicinity of the gold clusters, but in such a way that the corrugation of the potential is increased, i.e., the energy of the minima associated with CO-TiO_2 binding sites decreases faster than the energy of the barriers between sites. The deeper minima would increase the CO lifetime on the surface, but larger corrugation would slow the diffusion toward the clusters. Both CO oxidation activity and CO_2 temporal behavior would be influenced by the (cluster-size-dependent) diffusion barriers, and by the efficiency of the actual CO step, as in scenario 1. This is, essentially, a variant of scenario 1, differing only in CO spending significant time in binding sites near the clusters, rather than only trapping in association with the clusters.

(3) The CO oxidation reaction is only efficient for Au_3, Au_4, and Au_7 (the sites with delayed CO_2 peaks) when multiple CO molecules are at the active site, via some cooperative effect. For example, binding of a second CO might modify the electronic properties of the cluster such that the oxidation barrier is lowered. As noted above, the CO pulse intensity is such that the CO fluence ranges from ~ 1.5 to ~ 4 CO/cluster for Au_3-Au_7, so capture of multiple CO molecules is conceivable. This scenario also requires that CO has a long lifetime in association with the clusters, however, that probably would be true anyway if the CO-Au binding is strong enough to modify the Au catalytic properties. In this scenario, the activity would depend on the activity and how it is modified by CO for different size clusters, and the efficiency for capturing multiple CO molecules. The CO_2 temporal behavior would be influenced by both the CO capture kinetics and the kinetics of the CO oxidation step. A potential problem with this scenario is that if the first (nonreactive) CO is bound strongly to the clusters, then it may still be there during subsequent CO pulses. In this case, we would expect changes in the CO_2 temporal dependence during the first few pulses. None are observed. Furthermore, XPS after the CO oxidation experiments shows no sign of carbon contamination, although the sensitivity might not be high enough to see a single carbon atom on a fraction of the gold clusters.

Our experiments cannot directly distinguish between these scenarios or variations that might also rationalize the observed activity and CO_2 temporal behavior. Because it is simplest, we tend to favor scenario one. Additional theoretical work on the energy landscape for CO and O binding on and around Au_n/TiO_2 would be most helpful in understanding the mechanism for this reaction.

IV. SUMMARY

Room temperature CO oxidation activity was studied for $Au_n/TiO_2(110)$, $n=1-7$, under O_2-pre-dosed, pulsed CO conditions. Activity is strongly size dependent, first appearing for Au_3, declining to Au_5, then increasing substantially for Au_6 and Au_7. Activity is shown to be strongly correlated with the ability of the clusters to bind O_2 such that it attenuates Au ISS signal. Activity is not obviously correlated with CO binding or cluster morphology, at least for the conditions of our experiment. The ISS-visible, Au-bound oxygen is the limiting reactant under these conditions, and the total amount of CO_2 produced can be accounted for without invoking reaction of oxygen bound in or on the TiO_2 support. The evolution of CO_2 from the samples has temporal dependence that depends on cluster size, but the most active clusters do not necessarily have the fastest CO_2 evolution rates. Rather, the results suggest that the activity and temporal behavior under these conditions are controlled by a combination of the CO binding energy (i.e., desorption/diffusion rates) and the actual rate of the CO oxidation event.

ACKNOWLEDGMENTS

We gratefully acknowledge support by Grant No. DE-FG03-99ER15003 from the Chemical Sciences, Geosciences and Biosciences Division, Office of Basic Energy Sciences, Office of Science, U. S. Department of Energy.

[1] M. Haruta, Catal. Today **36**, 153 (1997).
[2] G. U. Kulkarni, C. P. Vinod, and C. N. R. Rao, in *Surface Chemistry and Catalysis*, edited by A. F. Carley, P. R. Vavies, G. J. Hutchings, and M. S. Spencer (Kluwer Academic/Plenum Publishers, New York, 2002), pp. 191.
[3] T. S. Kim, J. D. Stiehl, C. T. Reeves, R. J. Meyer, and C. B. Mullins, J. Am. Chem. Soc. **125**, 2018 (2003).
[4] S. Lee, C. Fan, T. Wu, and S. L. Anderson, J. Am. Chem. Soc. **126**, 5682 (2004).
[5] D. C. Meier, X. Lai, and D. W. Goodman, in *Surface Chemistry and Catalysis*, edited by A. F. Carley, P. R. Vavies, G. J. Hutchings, and M. S. Spencer (Kluwer/Plenum, New York, 2002), pp. 147.
[6] V. A. Bondzie, S. C. Parker, and C. T. Campbell, Catal. Lett. **63**, 143 (1999).
[7] M. Valden, X. Lai, and D. W. Goodman, Science **281**, 1647 (1998).
[8] A. Sanchez, S. Abbet, U. Heiz, W.-D. Schneider, H. Häkkinen, R. N. Barnett, and U. Landman, J. Phys. Chem. A **103**, 9573 (1999).
[9] B. Hammer and J. K. Norskov, Nature (London) **376**, 238 (1995).
[10] G. R. Bamwenda, S. Tsubota, T. Nakamura, and M. Haruta, Catal. Lett. **44**, 83 (1997).
[11] M. S. Chen and D. W. Goodman, Science **306**, 252 (2004).
[12] Q. Fu, H. Saltsburg, and M. Flytzani-Stephanopoulos, Science **301**, 935 (2003).
[13] B. Yoon, H. Haekkinen, U. Landman, A. S. Woerz, J.-M. Antonietti, S. Abbet, K. Judai, and U. Heiz, Science **307**, 403 (2005).
[14] H.-G. Boyen, G. Kästle, F. Weigl, B. Koslowski, C. Dietrich, P. Ziemann, J. P. Spatz, S. Riethmüller, C. Hartmann, M. Möller, G. Schmid, M. G. Garnier, and P. Oelhafen, Science **297**, 1533 (2002); J. M. Gottfried, K. J. Schmidt, S. L. M. Schroeder, and K. Christmann, Surf. Sci. **525**, 197 (2003).
[15] M. Aizawa, S. Lee, and S. L. Anderson, J. Chem. Phys. **117**, 5001 (2002).
[16] S. Lee, C. Fan, T. Wu, and S. L. Anderson, Surf. Sci. **578**, 5 (2005).
[17] S. Lee, C. Fan, T. Wu, and S. L. Anderson, J. Phys. Chem. **109**, 381 (2005).
[18] W. S. Epling, C. H. F. Peden, M. A. Henderson, and U. Diebold, Surf. Sci. **412/413**, 333 (1998).
[19] K. Judai, S. Abbet, A. S. Worz, M. A. Rottgen, and U. Heiz, Int. J. Mass. Spectrom. **229**, 99 (2003).

[20] M. Bowker, P. Stone, R. Bennett, and N. Perkins, Surf. Sci. **497**, 155 (2002).
[21] S. K. Buratto, private communication (2005).
[22] J. W. Rabalais, *Principles and Applications of Ion Scattering Spectrometry: Surface Chemical and Structural Analysis* (Wiley, New York, 2003).
[23] M. Aizawa, S. Lee, and S. L. Anderson, Surf. Sci. **542**, 253 (2003).
[24] O. Dulub, W. Hebenstreit, and U. Diebold, Phys. Rev. Lett. **84**, 3646 (2000).
[25] M. S. Chen and D. W. Goodman, Science 1102420 (2004).
[26] C. C. Chusuei, X. Lai, K. Luo, and D. W. Goodman, Top. Catal. **14**, 71 (2001).
[27] S. Lee, C. Fan, T. Wu, and S. L. Anderson, J. Phys. Chem. B **109**, 11340 (2005).
[28] L. M. Molina, M. D. Rasmussen, and B. Hammer, J. Chem. Phys. **120**, 7673 (2004).
[29] M. A. Henderson, W. S. Epling, C. L. Perkins, C. H. F. Peden, and U. Diebold, J. Phys. Chem. **103**, 5328 (1999).
[30] J. M. Pan, B. L. Maschhoff, U. Diebold, and T. E. Maday, J. Vac. Sci. Technol. A **10**, 2470 (1992).
[31] R. Schaub, E. Wahlström, A. Rønnau, E. Lægsgaard, I. Stensgaard, and F. Besenbacher, Science **299**, 377 (2003).
[32] R. Schaub, P. Thostrup, N. Lopez, E. Lægsgaard, I. Stensgaard, J. K. Nørskov, and F. Besenbacher, Phys. Rev. Lett. **87**, 266104 (2001); Y. Wang, D. Pillay, and G. S. Hwang, Phys. Rev. B **70**, 193410/1 (2004); X. Wu, A. Selloni, and S. K. Nayak, J. Chem. Phys. **120**, 4512 (2004); M. D. Rasmussen, L. M. Molina, and B. Hammer, J. Chem. Phys. **120**, 988 (2004).
[33] Z.-P. Liu, X.-Q. Gong, J. Kohanoff, C. Sanchez, and P. Hu, Phys. Rev. Lett. **91**, 266102 (2003).
[34] C. B. Mullins, private communication (2004).